DNTTIP1 promotes nasopharyngeal carcinoma metastasis via recruiting HDAC1 to DUSP2 promoter and activating ERK signaling pathway

Shirong Ding,[a,b] Ying Gao,[a] Dongming Lv,[d] Yalan Tao,[b] Songran Liu,[e] Chen Chen,[b] Zilu Huang,[b] Shuohan Zheng,[b] Yujun Hu,[b] Larry Ka-Yue Chow,[f] Yinghong Wei,[b] Ping Feng,[a,b] Wei Dai,[f] Xin Wang,[a,c,**] and Yunfei Xia[a,b,*]

[a]State Key Laboratory of Oncology in South China, Collaborative Innovation Center for Cancer Medicine, Guangdong Key Laboratory of Nasopharyngeal Carcinoma Diagnosis and Therapy, Sun Yat-sen University Cancer Center, Guangzhou, China
[b]Department of Radiation Oncology, Sun Yat-sen University Cancer Centre, Guangzhou, China
[c]Department of Liver Surgery, Sun Yat-sen University Cancer Centre, Guangzhou, China
[d]Department of Burn and Plastic Surgery, The First Affiliated Hospital of Sun Yat-sen University, Guangzhou, China
[e]Department of Pathology, Sun Yat-sen University Cancer Centre, Guangzhou, China
[f]Department of Clinical Oncology, University of Hong Kong, Hong Kong (SAR), China

Summary

Background Distant metastasis remains the leading cause of treatment failure in patients with nasopharyngeal carcinoma (NPC), making it critical to identify efficient therapeutic targets for metastatic NPC. Previous studies have demonstrated that deoxynucleotidyltransferase terminal-interacting protein 1 (DNTTIP1) is associated with the development of various types of cancer. However, its role and mechanism in NPC have not been explored.

Methods RNA-seq profiling was performed for three pairs of NPC and normal nasopharynx tissues. DNTTIP1 expression in NPC specimens was detected by immunohistochemistry. *In vitro* and *in vivo* assays were used to investigate the function of DNTTIP1. The molecular mechanism was determined using RT-qPCR, western blotting, RNA-seq, luciferase reporter assays, ChIP assays, and co-IP assays.

Findings DNTTIP1 was found to be significantly upregulated in NPC tissues. Furthermore, DNTTIP1 promoted NPC growth and metastasis *in vitro* and *in vivo*. Upregulation of DNTTIP1 in NPC indicated poor clinical outcomes. Mechanistically, DNTTIP1 suppressed *DUSP2* gene expression via recruiting HDAC1 to its promoter and maintaining a deacetylated state of histone H3K27. The downregulation of DUSP2 resulted in aberrant activation of the ERK signaling and elevated MMP2 levels, promoting NPC metastasis. Chidamide, an HDAC inhibitor, was shown to suppress NPC metastasis by regulating the DNTTIP1/HDAC1-DUSP2 axis.

Interpretation Our findings demonstrate that DNTTIP1 not only regulates NPC metastasis but also independently predicts NPC prognosis. Furthermore, targeting DNTTIP1/HDAC1 by Chidamide may benefit NPC patients with metastasis.

Funding This work was supported by the National Natural Science Foundation of China (No. 81872464, 82073243).

Keywords: Nasopharyngeal carcinoma; DNTTIP1; DUSP2; ERK signaling pathway; Tumor metastasis; Chidamide

eBioMedicine 2022;81: 104100
Published online xxx
https://doi.org/10.1016/j.ebiom.2022.104100

*Corresponding author at: Department of Radiation Oncology, Sun Yat-sen University Cancer Centre; State Key Laboratory of Oncology in South China, Sun Yat-Sen University Cancer Center, 651 Dongfeng Road East, Guangzhou 510060, China.
**Corresponding author at: State Key Laboratory of Oncology in South China, Department of Liver Surgery, Sun Yat-Sen University Cancer Center, 651 Dongfeng Road East, Guangzhou 510060, China.
E-mail addresses: wangxin1@sysucc.org.cn (X. Wang), xiayf@sysucc.org.cn (Y. Xia).

Introduction

Nasopharyngeal carcinoma (NPC), arising from the nasopharynx epithelium, is highly prevalent in Southeast Asia, especially in China.[1] More than 70% of new cases are diagnosed with locally advanced disease.[2,3] The promotion of intensity-modulated radiotherapy (IMRT) and concurrent chemoradiotherapy has significantly improved the prognosis of patients.[4,5] However, distant metastasis remains the

Research in context

Evidence before this study

Nasopharyngeal carcinoma (NPC) originates from the nasopharyngeal epithelium and is characterized by insidious symptoms and aggressiveness. Despite advances in clinical diagnosis and treatment, distant metastasis remains a major cause of treatment failure and cancer-related death for NPC patients. Therefore, it is important to identify potential therapeutic targets for NPC metastasis. Previous researches have shown that DNTTIP1 is involved in mitosis and the cell cycle, and has tumorigenic effects in a variety of tumors. However, the role of DNTTIP1 in regulating NPC progression and metastasis remains unknown.

Added value of this study

In this study, we found that DNTTIP1 could be a biomarker to predict the prognosis of NPC patients. Overexpression of DNTTIP1 recruited HDAC1 to deacetylate histone H3K27 at the DUSP2 promoter to transcriptionally suppress DUSP2. The downregulation of DUSP2 led to aberrant activation of the ERK signaling, which promoted NPC metastasis. This provides evidence that DNTTIP1 promotes cancer metastasis in NPC, and this function of DNTTIP1 is dependent on DUSP2. Furthermore, Chidamide, an HDAC inhibitor, could suppress NPC metastasis via regulating the DNTTIP1/HDAC1-DUSP2 axis.

Implications of all the available evidence

Our study reveals that DNTTIP1 is an independent risk factor that influences the prognosis of NPC, as well as a regulator that promotes NPC development and metastasis. Therefore, DNTTIP1 could be a promising therapeutic target. Thus, targeting DNTTIP1/HDAC1 by Chidamide has clinical potential in the treatment of NPC.

leading cause of treatment failure and cancer-related death in NPC patients.[6-8] Therefore, a better understanding of the molecular mechanisms of NPC metastasis and the development of potential therapeutic strategies is critical.

DNTTIP1 is a DNA-binding protein, which enhances the activity of terminal deoxynucleotidyltransferase (TdT), and promotes the polymerization of DNA in lack of DNA templates.[9,10] Recent researches have discovered that DNTTIP1 can form a complex with HDAC1/2 and MIDEAS in *Homo sapiens*, which is known as the mitotic deacetylase complex (MiDAC).[11] Throughout the cell cycle, all of the components of the MiDAC complex have been indicated to be specifically associated with, and be substrates of, CyclinA2/CDK2.[12] Consistent with the observation of the MiDAC complex in regulating cell proliferation, it has been implied that the participants of the MiDAC complex may contribute to the progression of human cancer.[13] Indeed, mounting evidence suggests that DNTTIP1 is linked to the development of various types of cancer. For example, elevated expression of DNTTIP1 in non-small-cell lung cancer is associated with enhanced tumorigenesis[14]; DNTTIP1 promotes tumor cell proliferation in oral squamous cell carcinomas by regulating the cell cycle[15]; and DNTTIP1 exhibits close relationships with myeloid-derived suppressor cell infiltration levels and various core cancer intrinsic CTLs-evasion genes.[16] However, whether DNTTIP1 is correlated with poor prognosis of cancer, and the mechanism underlining is largely unknown. Here, we report that a high level of DNTTIP1 is associated with poor outcomes in NPC. In mechanism, DNTTIP1 promotes NPC metastasis via recruiting HDAC1 to efficiently catalyze the deacetylation of histone H3K27 at the *DUSP2* promoter, which leads to the silencing of *DUSP2* gene and the activation of ERK signaling. This study may provide strategies to target NPC patients with metastasis.

Methods

Cell culture

The human nasopharyngeal carcinoma cell line HK1 and human cancer cell lines (HONE1, 5-8F and 6-10B) were cultured in RPMI-1640 (Invitrogen, Carlsbad, USA) supplemented with 10% fetal bovine serum (FBS, Gibco, Grand Island, NY, USA). The human immortalized nasopharyngeal epithelial cell lines (NP69) were cultured in keratinocyte/serum-free medium (Invitrogen) supplemented with bovine pituitary extract (BD Bioscience, San Diego, CA, USA). The above cell lines were generously provided by Dr. Musheng Zeng (Sun Yat-sen University Cancer Center). The human nasopharyngeal carcinoma cell line C666-1 was cultured in RPMI-1640 (Invitrogen, Carlsbad, USA) supplemented with 10% fetal bovine serum (FBS, Gibco, Australia). The work relevant to C666-1 cell line was performed in collaboration with Dr. Wei Dai (University of Hong Kong). In addition, the HEK293T embryonic kidney cells were obtained from the American Type Culture Collection (ATCC), they were cultured in DMEM supplemented with 10% FBS. All cell lines were cultured at 37°C and 5% CO_2 and were regularly tested for mycoplasma contamination.

Plasmid construction

The Flag-tagged HDAC constructs were gifts from Prof. Binhua P. Zhou (University of Kentucky). *DNTTIP1* was cloned into the pSIN-EF2-puro vector. The promoter regions of *DNTTIP1* and *DUSP2* were cloned

into the pGL3-basic vector. The PLKO.1-puro vector was used to clone the shRNAs that target *DNTTIP1* and *DUSP2*. The sequences used for cloning the indicated shRNAs are reported in Supplementary Materials and Methods.

RNA extraction and qRT-PCR

Briefly, total RNA was isolated using TRIzol reagent (Invitrogen) according to the manufacturer's instructions. First-strand cDNA was synthesized using the Revert AidTM First Strand cDNA Synthesis Kit (MBI Fermentas). The primers used to amplify the indicated genes are shown in Supplementary Materials and Methods.

RNA-seq

RNA-seq of three pairs of nasopharyngeal carcinoma tissues and normal nasopharynx tissues was performed by Novogene using Illumina X TEN. The 6GB clean data per sample were collected for RNA-seq. Hg38 assembly was used for the read alignment, and gene annotation was obtained using Ensembl gene annotation version 90. RNA-seq of DNTTIP1 knockdown was performed by Novogene using Illumina NovoSeq 6000. The 6 GB clean data per sample were collected for RNA-seq, and the clean reads were aligned to the human genome GRCh38 (Hg38) using hisat2 (version 2.0.5).

RNAi treatment

Transfection was performed according to the manufacturer's instructions using Lipofectamine RNAi MAX transfection reagent (Invitrogen) and 50 nM siRNA. The oligonucleotide sequences are shown in Supplementary Materials and Methods.

The luciferase reporter assay

Briefly, the cells were plated in 12-well plates at a density of 1.2×10^5 cells per well then transfected with 0.5μg of a promoter-luciferase plasmid. To normalize the transfection efficiency, the cells were also co-transfected with 5ng of pRL-CMV (Renilla luciferase). After 48 hours post-transfection, the luciferase activity was measured using a Dual-Luciferase Assay kit (Promega). Three independent experiments were performed, and the calculated means and standard deviations are obtained. The primer used for cloning the *DUSP2* and *DNTTIP1* promoter was shown in Supplementary Materials and Methods.

Western blotting and Co-immunoprecipitation (Co-IP)

Briefly, cells were collected and lysed by RIPA buffer (150mM NaCl, 0.5% EDTA, 50mM Tris, 0.5% NP40) and centrifuged for 20 min at 12000 rpm and 4°C. Fifty micrograms of harvested total protein were loaded and separated on a 10% sodium dodecyl sulfate-polyacrylamide gradient gel. The gels were transferred to Immobilon-P PVDF membranes (Millipore), which were then blocked in PBS with 5% nonfat milk and 0.1% Tween-20 and probed with primary antibodies overnight at 4° C. Secondary HRP-conjugated antibodies were used, and clarity ECL substrate (Bio-Rad) or high-sig ECL substrate (Tanon) was used for detection by MiniChmei Chemiluminescence imager (SAGECREATION, Beijing).[17]

To investigate the interaction between endogenous DNTTIP1 and HDAC1, the clarified supernatants were first incubated with an anti-DNTTIP1 antibody for 2 hours at 4°C. Protein A/G-agarose was then added overnight, and the precipitates were washed five times with RIPA and analyzed by western blotting. The antibodies used in this work are shown in Supplementary Materials and Methods.

The chromatin immunoprecipitation (ChIP) assay

This procedure was performed as described by the ChIP kit (Millipore, 17-10085& 17-10086). Briefly, 15 cm plates were seeded with cells of tested cell lines and allowed to grow to 70-80% confluence. Complete Cell Fixative Solution (1/10 the volume of growth medium volume) was added to the existing culture medium to fix cells. The fixation reaction was stopped by adding Stop Solution (1/20 the volume of growth medium volume) to the existing culture medium. The cells were collected by centrifugation, and the nuclear pellet was resuspended in ChIP Buffer. The cell lysate was subjected to sonication and then incubated with 5μg of antibodies overnight, followed by incubation with the protein A/G agarose beads overnight at 4°C. Bound DNA-protein complexes were eluted, and cross-links were reversed after a series of washes. The purified DNA was resuspended in TE buffer for PCR. The primers for the indicated promoters are shown in Supplementary Materials and Methods.

Migration and invasion assays

Transwell assays using Boyden chambers containing 24-well Transwell plates (BD Inc., USA) with 8μm pore size was used to evaluate the migration and invasiveness of cells. All experiments were performed in duplicate and repeated three times. For the migration assay, the cell culture inserts were seeded with 0.5×10^5 (5-8F, 6-10B or HONE1 cells) or 1.5×10^5 (HK1 or C666-1 cells) in 100μL of serum-free culture medium without an extracellular matrix coating. A culture medium containing 10% FBS was added to the bottom chamber. After 20 hours of incubation, the cells on the lower surface of the filter were fixed, stained, and examined using a microscope. For the invasion assay, the membrane was coated with 50μL of 1:8 diluted Matrigel (BD

Biosciences, USA). After the Matrigel had solidified at 37°C for 2 hours, 0.5×10^5 (5-8F, 6-10B or HONE1 cells) or 1.5×10^5 (HK1 or C666-1 cells) in 100μL of serum-free culture medium were added to the cell culture inserts, whereas the lower chamber was filled with culture medium containing 20% FBS. The Boyden chamber was then incubated at 37°C in 5% CO_2 for 24 hours. The cells were then stained and observed as described for the migration assays.[18]

Animal experiments

Animal care and experiments were performed in strict accordance with the "Guide for the Care and Use of Laboratory Animals" and the "Principles for the Utilization and Care of Vertebrate Animals" and were approved by the Animal Research Committee of Sun Yat-sen University Cancer Center (L102012018003Z).

Four-week-old male BALB/c nude mice were purchased from Jiangsu GemPharmatech Lab Animal Technology Co., LTD. The mice were randomly divided into 8 in each group after being bred for one week. For the lymph node metastasis model, 2×10^5 HONE1 cells were injected into the BALB/c nude mice footpads (n= 8 per group). After six weeks, the mice were killed, and the footpad tumors and the popliteal lymph nodes were excised for analysis. All the dissected tissue samples were paraffin-embedded, sectioned, and stained with H&E. For the lung metastasis model, 1×10^6 HONE1 or HK1 cells were injected into the tail veins of the mice. After six weeks, the mice were killed and the lung tissue was fixed and paraffin-embedded for H&E staining. For the lymph node metastasis model or the lung metastasis model following Chidamide treatment, HONE1 or HK1 cells were injected into the footpads or tail veins of mice. One week later, Chidamide was formulated in 1% CMC Na and was used at 20 mg/kg every two days by intragastric administration for five weeks. Their respective vehicles were used as the controls.

Human tissue specimens

For prognosis analysis, 96 paraffin-embedded NPC biopsy tissues were collected from NPC patients with detailed clinical characteristics and long-term follow-up data at Sun Yat-sen University Cancer Center (China). For expression analysis, another 83 freshly-frozen NPC samples were obtained from Sun Yat-sen University Cancer Center. None of the patients received any antitumor therapy before a biopsy. This study was approved by the Institutional Ethical Review Board of Sun Yat-sen University Cancer Center (GZR2018-100), and written informed consent was obtained from all patients.

Immunohistochemistry staining (IHC)

IHC staining was performed on 3μm sections. The primary antibodies against DNTTIP1 were diluted at 1:50, respectively, and then incubated at 4°C overnight in a humidified container. After three washes with PBS, the tissue slides were treated with a non-biotin horseradish peroxidase detection system according to the manufacturer's instructions (Dako). The IHC staining was evaluated by two independent pathologists without knowledge of the clinical outcome. The protein expression levels of DNTTIP1 were evaluated based on thirteen scores. Generally, the DNTTIP1 signals were detected in the nucleus. To evaluate DNTTIP1, a semi-quantitative scoring criterion was used and both staining intensity and positive areas were recorded. A staining index (values 0–12), which was obtained as the product of intensity of positive staining (weak, 1; moderate, 2; strong, 3) and the proportion of immunopositive cells of interest (0%, 0; <10%, 1; 10–50%, 2; 51–80%, 3; >80%, 4), was calculated. The immunohistochemical cut-off for high or low expression of the indicated molecule was determined through the ROC curve analysis. The sensitivity and specificity for discriminating dead or alive were plotted as IHC score, thus generating a ROC curve. The cut-off value was established to be the point on the ROC curve where the sum of sensitivity and specificity was maximized. Cancers with scores above the obtained cut-off value were considered to have high expression of the indicated molecule and vice versa.

Statistical analysis

Patient data analysis. In this study, overall survival (OS) was defined as the period between the date of diagnosis to death due to any cause. Progression-free survival (PFS) was defined as the time from the date of diagnosis to withdrawal from the study due to progression or death. Distant metastasis-free survival (DMFS) was defined as the time from the date of diagnosis to withdrawal from the study due to distant metastasis or death. The correlations between DNTTIP1 expression and overall, progression-free, distant metastasis-free survival curves were assessed using Kaplan-Meier plots and compared with the log-rank test. Multivariate analysis was carried out using the Cox regression model. $p < 0.05$ was considered statistically significant.

Experiments data analysis. The SPSS software (version 16.0, SPSS Inc., Chicago, IL, USA) was used for the statistical analysis. The significance of differences was assessed using a two-tailed Student's t-test or a chi-squared test, as appropriate. $p < 0.05$ was considered statistically significant. * $p < 0.05$, ** $p < 0.01$, *** $p < 0.001$.

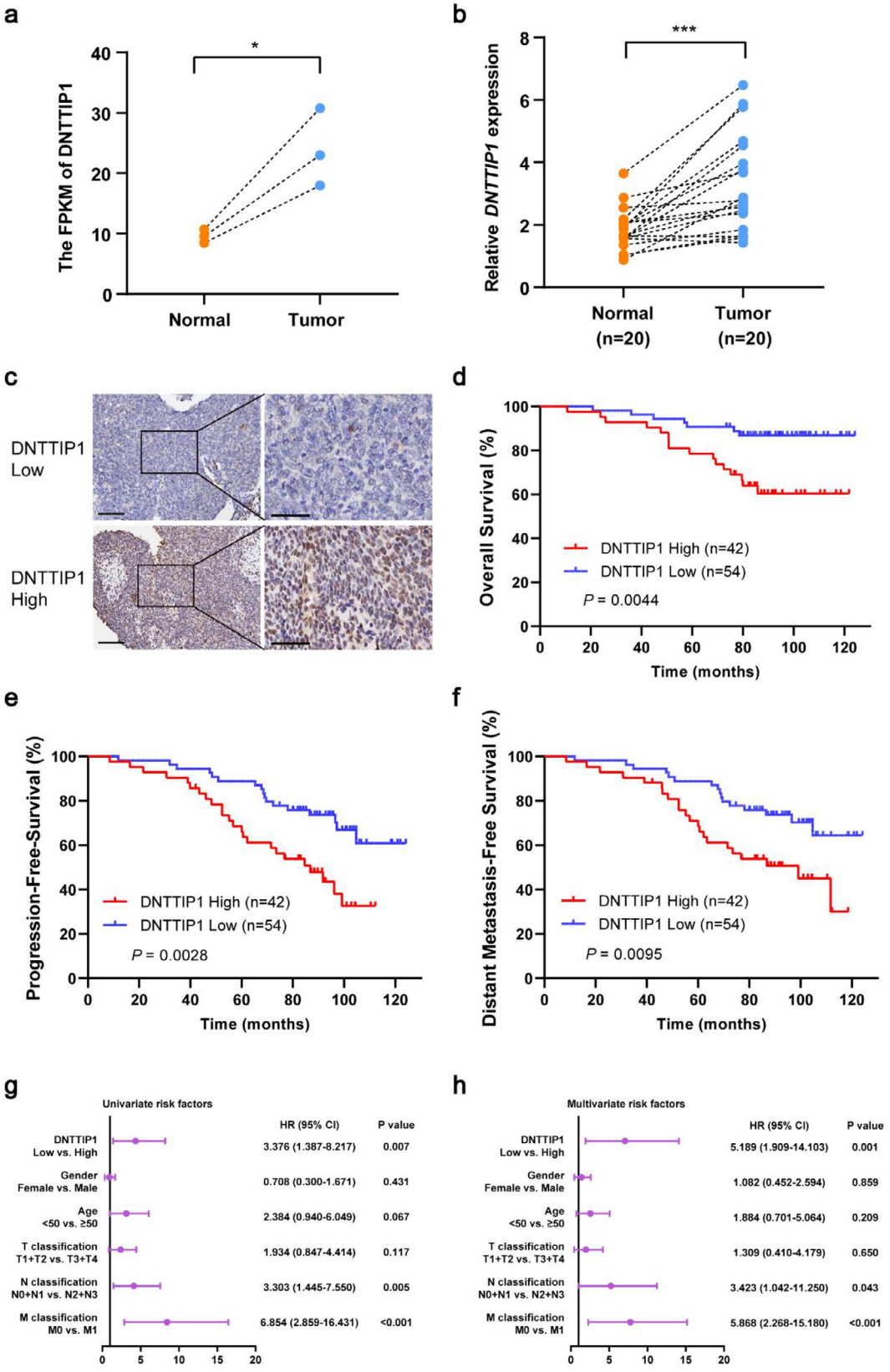

Figure 1. DNTTIP1 is highly expressed in NPC and associated with poor prognosis. (a) The FPKM (fragments per kilobase million) of DNTTIP1 in 3 pairs of normal nasopharyngeal epithelial tissues and nasopharyngeal carcinoma tissues. * $p < 0.05$ using

Study approval

The animal experiments were approved by the Animal Research Committee of Sun Yat-sen University Cancer Center and were performed in accordance with established guidelines. The use of human nasopharyngeal carcinoma tissues was reviewed and approved by the ethical committee of Sun Yat-sen University Cancer Center, and informed consent was obtained from patients. The samples were retrospectively acquired from the department of radiation oncology archives of Sun Yat-sen University Cancer Center.

Role of funding sources

Funders had no role in study design, data collection, data analyses, interpretation, or the writing of this report. The author Shirong Ding and Xin Wang has directly accessed and verified the underlying data in the study. The corresponding author Yunfei Xia and Xin Wang had full access to all the data in the study and had final responsibility for the decision to submit the manuscript for publication.

Results

DNTTIP1 is overexpressed in nasopharyngeal carcinoma and correlates with poor clinical outcomes

To identify potential factors that may drive the progression of NPC, RNA-seq was performed in 3 pairs of NPC and normal nasopharynx tissues. We found that *DNTTIP1* was significantly overexpressed in NPC tissues compared with normal tissues (Figure 1a). Consistently, the mRNA level of *DNTTIP1* was also upregulated in NPC tissues compared to normal nasopharynx tissues in the other 20 samples of patients (Figure 1b). In addition, DNTTIP1 expression was higher in NPC cell lines than in the immortalized nasopharyngeal epithelial cell line NP69 (Supplemental Figure 1a-b). These results indicate that DNTTIP1 may play a crucial role in the progression of NPC. Indeed, the immunohistochemical (IHC) staining was performed in 96 NPC tissues with an anti-DNTTIP1 antibody, which indicated that DNTTIP1 localized in the nucleus (Figure 1c). Kaplan-Meier survival analysis revealed that patients with a high level of DNTTIP1 had poorer outcomes in both overall, progression-free and distant metastasis-free survival (Figure 1d–f). Furthermore, Chi-square (χ^2) test showed that DNTTIP1 level was most significantly associated with progression (p=0.012), distant metastasis (p=0.024), and vital status (p=0.004; Supplementary Table S1). Moreover, the univariate and multivariate analyses revealed that the DNTTIP1 expression level (p=0.001), with an HR of 5.189 and a 95% CI of 1.909-14.103, was an independent prognostic factor for NPC patients (Figure 1g–h). These results indicate that DNTTIP1 may be related to the progression and metastasis of cancer, and may serve as a new marker to predict clinical outcomes of NPC patients.

DNTTIP1 promotes tumor progression and metastasis in NPC

To demonstrate whether DNTTIP1 promotes the cell proliferation, the expression of DNTTIP1 was knocked down by two pairs of small hairpin RNA (shRNA) in HK1, HONE1, and 5-8F cell lines or by two pairs of small interfering RNA (siRNA) in C666-1 cell line. Knockdown of DNTTIP1 reduced cell viability and soft agar colony formation ability in these cell lines (Figure 2a-d and Supplemental Figure 2a-d). Consistently, cell viability and soft agar colony formation ability were enhanced in HK1 and 6-10B stably overexpressing DNTTIP1 (Figure 2e-f and Supplemental Figure 2e-f). In addition, overexpressing DNTTIP1 dramatically increased tumor volume and weight when HK1 cells were inoculated into the armpit of nude mice (Figure 2g-i). However, these functions were reduced by knockdown of DNTTIP1 expression in HK1 or HONE1-cells (Figure 2j–l and Supplemental Figure 2g-i). These findings indicate that DNTTIP1 promotes NPC cell proliferation and tumor growth.

To identify the potential role of DNTTIP1 in tumor metastasis, we performed transwell assay to assess the cell motility. Knockdown of DNTTIP1 reduced migration and invasion ability in HK1, C666-1, HONE1, and 5-8F cell lines (Figure 3a-b and Supplemental Figure 3a-b), while overexpression of DNTTIP1 enhanced these functions in HK1 and 6-10B cell lines (Figure 3c and Supplemental Figure 3c). In *vivo*, when HONE1 cells were injected into the foot-pads of nude mice, the volumes of the popliteal lymph nodes were smaller, and the popliteal lymph node metastasis ratio was lower in the DNTTIP1-silenced group (Supplemental Figure 3d-h). To further evaluate the effect of DNTTIP1 on distant metastasis, we developed an *in vivo* lung metastasis

Student's t-test. **(b)** The relative mRNA levels of *DNTTIP1* were normalized to the *GAPDH* level in NPC tissue and normal nasopharyngeal epithelial tissue as determined by qRT-PCR. *** $p < 0.001$ using Student's *t*-test. **(c)** Representative images showing high or low expression of DNTTIP1 in NPC tumor specimens. (left, scale bar: 100μm; right, scale bar: 50μm) **(d-f)** Kaplan-Meier overall, progression-free and distant metastasis-free survival curves were generated based on the protein level of DNTTIP1 in 96 paraffin-embedded NPC tissues. Data were compared using log-rank test. **(g-h)** Univariate and multivariable analyses were performed in the NPC cohort. Data were compared using Cox proportional hazards models.

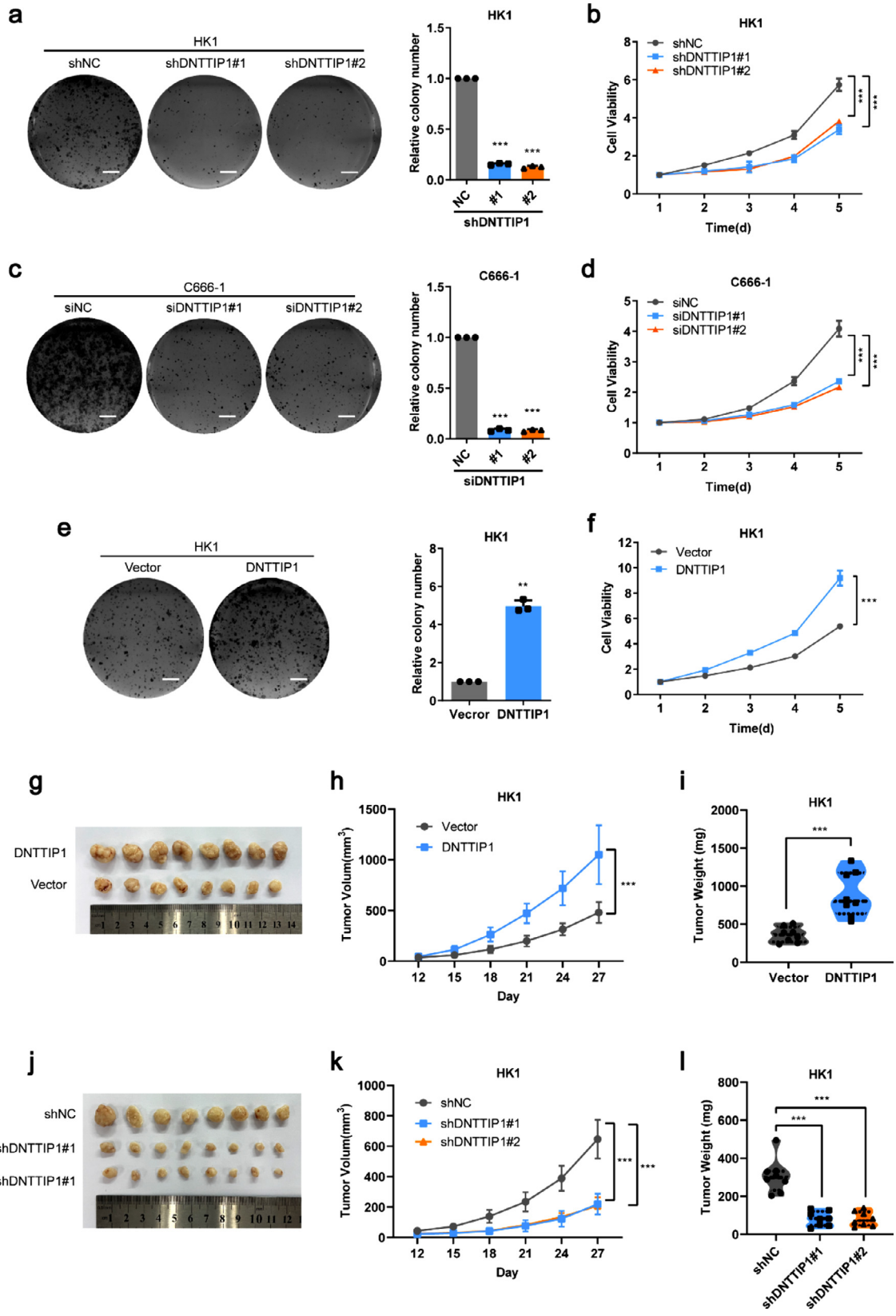

Figure 2. DNTTIP1 promotes NPC proliferation *in vitro* and *in vivo*. (a, c, e) Colony formation of the indicated stable cells. Representative data of three independent experiments. Scale bar: 5mm. Data are represented as the mean ± SD. ** $p < 0.01$, *** $p <$

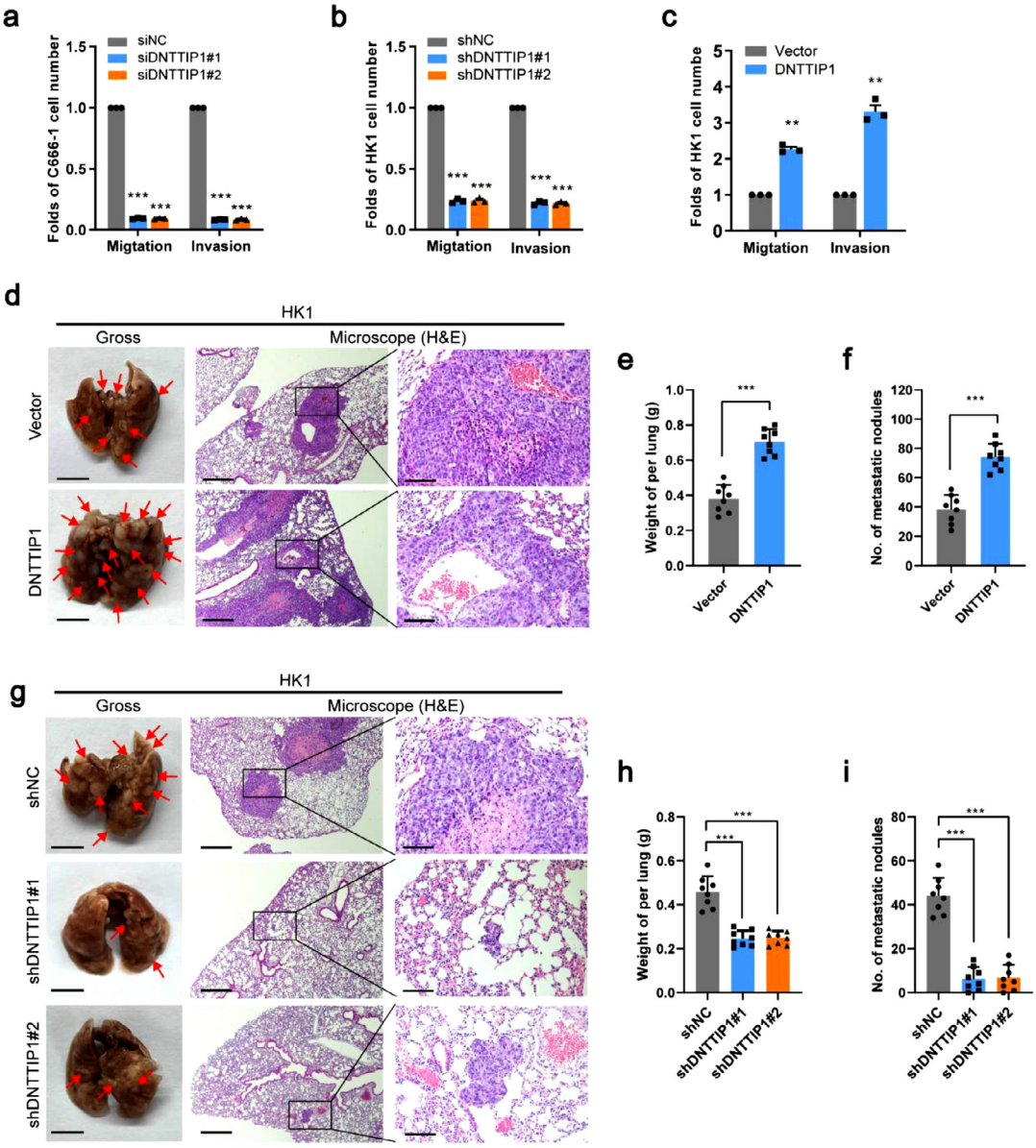

Figure 3. DNTTIP1 enhances cell migration, invasion, and metastasis of NPC. (a-c) Migration and invasion abilities were determined using the indicated stable cells. Representative data of three independent experiments. Data are represented as the mean ± SD. ** $p < 0.01$, *** $p < 0.001$ using Student's *t*-test. **(d-i)** The indicated stable cells were injected into the tail vein of BALB/c nude mice to construct a lung metastasis model (n=8 per group). General views (left, scale bar: 5mm) and H&E staining of lung tissues of the mouse models with the indicated cells (middle, scale bar: 500μm; right, scale bar: 100μm). The red arrows indicate macroscopic pulmonary nodules **(d, g)**. Lung weight **(e, h)**, and quantification of macroscopic metastatic nodules **(f, i)**. Data are represented as the mean ± SD. *** $p < 0.001$ using Student's *t*-test.

0.001 using Student's *t*-test. **(b, d, f)** Cell proliferation of the indicated stable cells. Representative data of three independent experiments. Data are represented as the mean ± SD. *** $p < 0.001$ using Student's *t*-test.**(a-d)** Colony formation and cell proliferation of DNTTIP1 knockdown HK1 and C666-1 cells. Representative data of three independent experiments. Data are represented as the mean ± SD. *** $p < 0.001$ using Student's *t*-test. **(e-f)** Colony formation and cell proliferation of DNTTIP1 overexpressing HK1 cells. Representative data of three independent experiments. Data are represented as the mean ± SD. ** $p < 0.01$, *** $p < 0.001$ using Student's *t*-test. **(g-l)** General view, tumor volume, and tumor weight in xenograft mouse models with DNTTIP1 overexpression or knockdown HK1 cells (n=8 per group). Data are represented as the mean ± SD. *** $p < 0.001$ using Student's *t*-test.

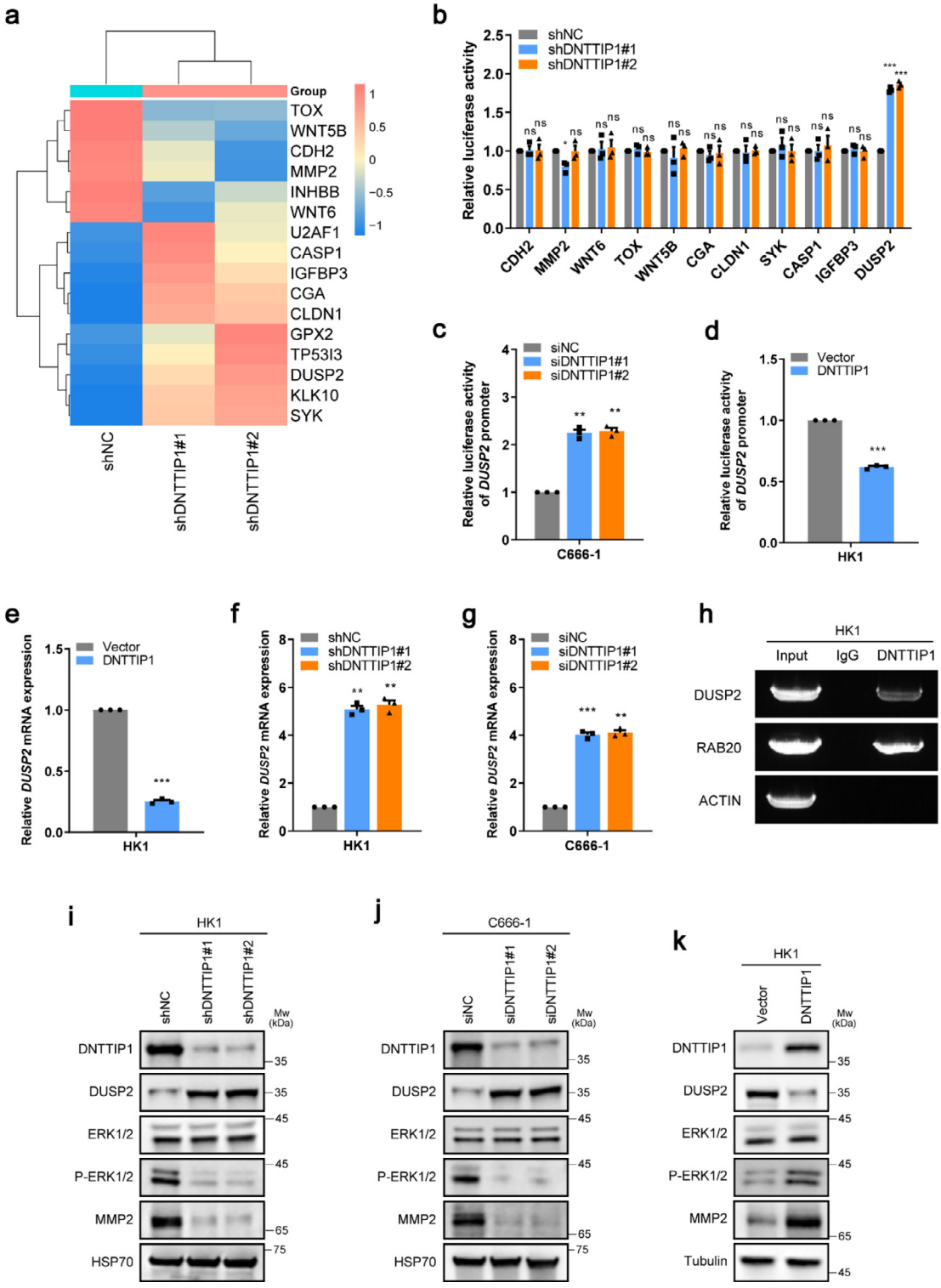

Figure 4. DNTTIP1 directly downregulates *DUSP2* by occupying its promoter. (a) Representative heatmaps from global comparative transcriptome analysis indicating genes regulated upon DNTTIP1-knockdown. **(b-d)** The indicated stable cells transfected with the DUSP2-Luc reporter for 48h were subjected to the luciferase activity assay. Representative data of three independent experiments. Data are represented as the mean ± SD. ** $p < 0.01$, *** $p < 0.001$, ns, no significance using Student's *t*-test. **(e-g)** The relative mRNA levels of the indicated genes were normalized to the *GAPDH* level in the indicated stable cells as determined by qRT-PCR.

model by injecting tumor cells into the lateral tail vein of mice. Ectopic expression of DNTTIP1 resulted in a significant increase of lung weight and numbers of metastatic pulmonary nodules (Figure 3d-f), while knockdown reduced these parameters (Figure 3g-i and Supplemental Figure 3i-k). These results suggest that DNTTIP1 plays an oncogenic role in NPC metastasis.

DNTTIP1 occupies the *DUSP2* promoter and represses its expression

As a transcription regulator, DNTTIP1 may target downstream genes and mediate their epigenetic modification.[19] To investigate the molecular mechanism of DNTTIP1 in NPC, the global transcriptomes were analyzed in DNTTIP1-silenced cells compared with scrambled cells (Figure 4a). Intriguingly, the expression of factors that are well known to be related to proliferation and metastasis, such as WNT6, CDH2, MMP2, and DUSP2, were altered by knocking down DNTTIP1, which were also proved by the qRT-PCR assay in these cells (Supplementary Figure S4a). Therefore, a luciferase reporter assay was then used to further identify the direct downstream target of DNTTIP1. Among the genes shown in Supplementary Figure S4a, only the promoter activity of DUSP2 was significantly increased upon DNTTIP1 knockdown (Figure 4b-c and Supplementary Figure S4b-c). Accordingly, the overexpression of DNTTIP1 decreased DUSP2 promoter activity (Figure 4d and Supplementary Figure S4d). Furthermore, DNTTIP1 overexpression or knockdown decreased or increased the level of DUSP2, respectively (Figure 4e-g and Supplementary Figure S4e-g). Moreover, DNTTIP1 was associated with the *DUSP2* promoter according to a chromatin immunoprecipitation (ChIP) assay (Figure 4h and Supplementary Figure S4h). Previous studies have demonstrated that DUSP2 is a negative regulator of p-ERK1/2.[20,21] Here, we observed that knockdown of DNTTIP1 could increase DUSP2 and decrease p-ERK1/2 and MMP2 in the protein level (Figure 4i-j and Supplementary Figure S4i-j). Consistently, overexpression of DNTTIP1 could downregulate DUSP2 and upregulate p-ERK1/2 and MMP2 (Figure 4k and Supplementary Figure S4k). Taken together, these data indicate that DNTTIP1 downregulates DUSP2 by occupying the *DUSP2* promoter and induces the activation of ERK signaling.

HDAC1 associates with DNTTIP1 and specifically represses the *DUSP2* promoter via histone deacetylation

It has been reported that DNTTIP1 participates in the MiDAC complex to mediate the deacetylation of downstream targets.[19] As expected, the ChIP assay showed that knockdown of DNTTIP1 had little effect on the binding of H3K27-Me3 to the *DUSP2* promoter in HK1 and HONE1 cells. However, using RNA polymerase II (PolII) as the positive control, the association of H3K27-Ac to the *DUSP2* promoter was enhanced by knocking down DNTTIP1 in these cells (Figure 5a and Supplementary Figure S5a). In consideration of HDAC1/HDAC2 being the core deacetylases in the MiDAC complex, we attempted to identify whether HDAC1 and/or HDAC2 may regulate the *DUSP2* promoter. As shown in Figure 5b-e and Supplementary Figure S5b-e, HDAC1, but not HDAC2, dramatically reduced the promoter activity, mRNA level, as well as protein expression of DUSP2. In addition, the direct protein binding of DNTTIP1 to HDAC1 was already evidenced at endogenous levels (Figure 5f and Supplementary Figure S5f). Furthermore, knockdown of DNTTIP1 not only abolished the binding of HDAC1 to the *DUSP2* promoter but also abrogated the inhibition of *DUSP2* promoter activity mediated by HDAC1 overexpression (Figure 5g-h and Supplementary Figure S5g-h). Moreover, silencing HDAC1 reversed the suppression of H3K27-Ac and DUSP2, as well as the enhancement of migration and invasion, mediated by overexpression of DNTTIP1 in HK1 cells (Figure 5i-j). Therefore, HDAC1 is essential for the function of DNTTIP1 in NPC. To further illustrate the correlation between the expression of DNTTIP1 and DUSP2, RT-qPCR analysis was performed in 70 NPC tissues, and a negative correlation between them was observed (Figure 5k). In addition, western blotting analysis was conducted in 10 NPC tissues and showed a similar negative correlation (Figure 5l). Collectively, these results demonstrate that DNTTIP1 represses DUSP2 expression by recruiting HDAC1 to sustain the deacetylation status of H3K27 at the *DUSP2* promoter.

The oncogenic effect of DNTTIP1 on nasopharyngeal carcinoma depends on DUSP2

Then we explore whether the effect of DNTTIP1 on NPC cell migration and invasion depends on DUSP2. Both p-ERK1/2 and MMP2 protein levels, as well as cell migration and invasion promoted by overexpression of DNTTIP1, were reduced by further DUSP2 overexpression in HK1

Representative data of three independent experiments. Data are represented as the mean ± SD. ** $p < 0.01$, *** $p < 0.001$ using Student's *t*-test. **(h)** The ChIP assay was performed with HK1 cells using an anti-DNTTIP1 antibody or IgG antibody, as indicated. The RAB20 and ACTIN promoters were used as the positive and negative controls, respectively. These results are repeated in three independent experiments. **(i-k)** The indicated proteins were analyzed by Western blotting in the indicated stable cells. Western Blot bands were derived from three separate experiments but only one representative loading control is shown.

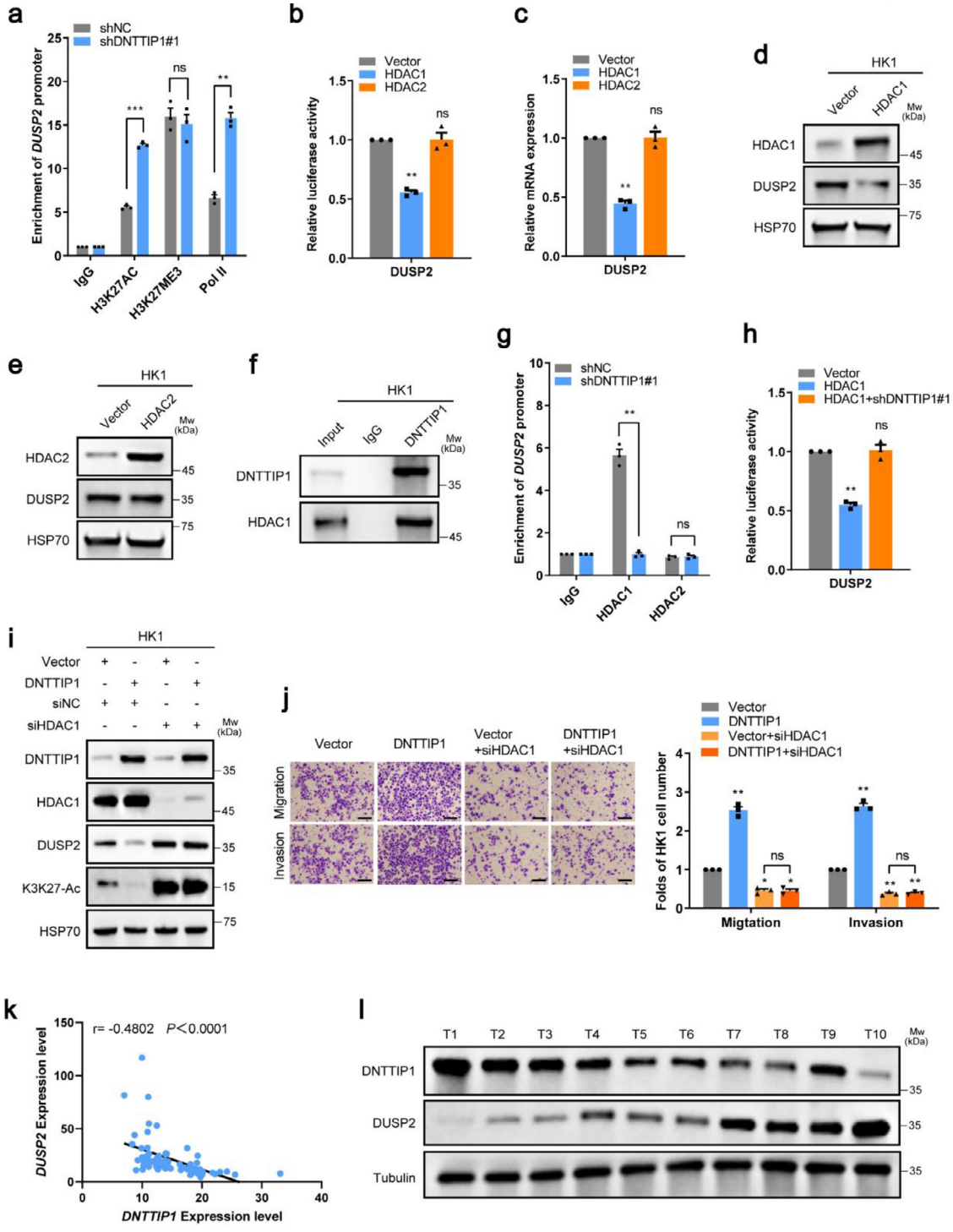

Figure 5. DNTTIP1 recruits HDAC1 to suppress the expression of *DUSP2*. **(a)** The ChIP-qPCR analysis of the occupancies of H3K27-Ac, H3K27-Me3, and Pol II on the *DUSP2* promoter in HK1 cells stably expressing control or shRNA-DNTTIP1. **(b, h)** The indicated stable cells transfected with the DUSP2-Luc reporter for 48h were subjected to the luciferase activity assay. **(c)** The relative mRNA levels of *DUSP2* were normalized to the *GAPDH* level in the indicated stable cells as determined by qRT-PCR. **(d-e, i)** The indicated proteins were analyzed by Western blotting in the indicated stable cells. **(f)** The co-IP assay was performed in HK1 cells expressing endogenous levels of DNTTIP1 using anti-DNTTIP1 antibody or anti-IgG antibody as indicated. **(g)** The ChIP-qPCR analysis of the occupancies of HDAC1 or HDAC2 on the *DUSP2* promoter in HK1 cells stably expressing control or shRNA-DNTTIP1.

and 6-10B cells (Figure 6a-b and Supplementary Figure S6a-b). In addition, knockdown of DNTTIP1 inhibited the protein level of p-ERK1/2 and MMP2 and the migration and invasion abilities of HK1, HONE1 and 5-8F cells, which could be reversed by further knocking down DUSP2 (Figure 6c-d and Supplementary Figure S6c-f). Subsequently, we explored the functional role of the DNTTIP1-DUSP2 axis in both the popliteal lymph node metastasis model and the lung metastasis model. Loss of DNTTIP1 reduced the popliteal lymph node metastasis ratio and the number of lung metastatic nodules, which could be reversed by DUSP2 silencing (Supplementary Figure S7). However, ectopic expression of DUSP2 abolished the enhancement of lung metastatic function induced by DNTTIP1 overexpression (Figure S6e-g). In summary, the oncogenic role of DNTTIP1 on NPC is dependent on the suppression of DUSP2.

Chidamide, an HDAC inhibitor, has the potential to against NPC metastasis

It has been reported that certain HDAC inhibitors have a high affinity for the MiDAC complex, and can even affect DNTTIP1 expression level.[11,15] We found that the class I HDAC inhibitor Chidamide (Tucidinostat, an NMPA-approved drug for the treatment of peripheral T cell lymphoma and breast cancer[22,23]) could upregulate the level of H3K27-Ac and DUSP2, downregulate the level of DNTTIP1, p-ERK and MMP2 (Figure 7a-b and Supplementary Figure S8a-b), and inhibit the proliferation, migration, and invasion of NPC cells (Figure 7c-f and Supplementary Figure S8c-f). Furthermore, using the popliteal lymph node metastasis model and the lung metastasis model, both the popliteal lymph node metastasis rate and the number of lung metastatic nodules were decreased in the Chidamide treatment group (Figure 7g-i and Supplementary Figure S8g-m). Moreover, after Chidamide treatment, the DNTTIP1 expression was decreased in xenografted tumors (Figure 7j and Supplementary Figure S8n). Therefore, the HDAC inhibitor Chidamide has the potential clinical application value for NPC patients with metastasis.

Discussion

In this study, as illustrated in Figure 8, we demonstrate that overexpression of DNTTIP1 may recruit HDAC1 to deacetylate histone H3K27 at the *DUSP2* promoter to transcriptionally suppress *DUSP2*. Downregulation of DUSP2 causes aberrant activation of the ERK signaling, which promotes NPC metastasis. This provides evidence that DNTTIP1 promotes cancer metastasis in NPC, and this function of DNTTIP1 is dependent on DUSP2. Furthermore, DNTTIP1 can be a biomarker to predict the prognosis of NPC patients.

Class I histone deacetylases, including HDAC1-3, are important epigenetic regulators.[24,25] These enzymes are always recruited to chromatin by protein complexes, such as NuRD, CoREST, and SMRT/NCoR complexes, to modify the acetylation state of histones.[26,27] In addition to HDACs, scaffold proteins, which are directly associated with transcription factors and target genes, determine the specificity of these complexes.[28,29] The MiDAC complex, which consists of three members: HDAC1/2, MIDEAS, and DNTTIP1, was discovered through a chemoproteomic profiling study due to its increased association with certain HDAC inhibitors in mitotically arrested cells versus non-synchronized proliferating cells.[11] The amino-terminal region of DNTTIP1 acts as a scaffold, mediating its interaction and assembly with HDAC1/2 and MIDEAS. The catalytic sites of HDAC are located at the extremities of the complex, suggesting that this complex could simultaneously target multiple nucleosomes and exert a highly processive deacetylation effect.[19,30,31] However, the MiDAC complex appears to lack regions that recruit specific transcription factors, and likely directly target nucleosomes through the DNTTIP1 DNA-binding domain.[13] Therefore, DNTTIP1 is playing a critical role in mediating the MiDAC complex to specific targets. Herein, we showed that DNTTIP1 recruited HDAC1, but not HDAC2, and suppressed the expression of DUSP2 by binding its promoter, consequently facilitating NPC progression and metastasis. These findings suggest that the MiDAC complex generated by DNTTIP1 and HDAC1 is pivotal for metastasis functions in NPC, thus HDAC1 inhibitors or small molecular inhibitors that impair the interaction between DNTTIP1 and HDAC1 may benefit NPC patients with metastasis.

Chidamide, an innovative new inhibitor of HDAC1, 2, 3, 10, was approved by the China Food and Administration (CFDA) for the treatment of relapsed Peripheral T cell lymphomas in 2014, and by the National Medical Products Administration (NMPA) for the treatment of breast cancer in 2019.[22,23] In addition, Chidamide has been reported to have significant antitumor activity in a

(j) Migration and invasion abilities were determined using the indicated stable cells. Scale bar: 50μm. **(k)** The correlation between *DNTTIP1* and *DUSP2* expression in 70 NPC tissues. **(l)** Correlation between DNTTIP1 and DUSP2 protein levels in 10 NPC tissues according to Western blotting. **(a-c, g, h, j)** Representative data of three independent experiments. Data are represented as the mean ± SD. * $p < 0.05$, ** $p < 0.01$, *** $p < 0.001$, ns, no significance using Student's *t*-test. **(d-f, i, l)** Western Blot bands were derived from three separate experiments but only one representative loading control is shown.

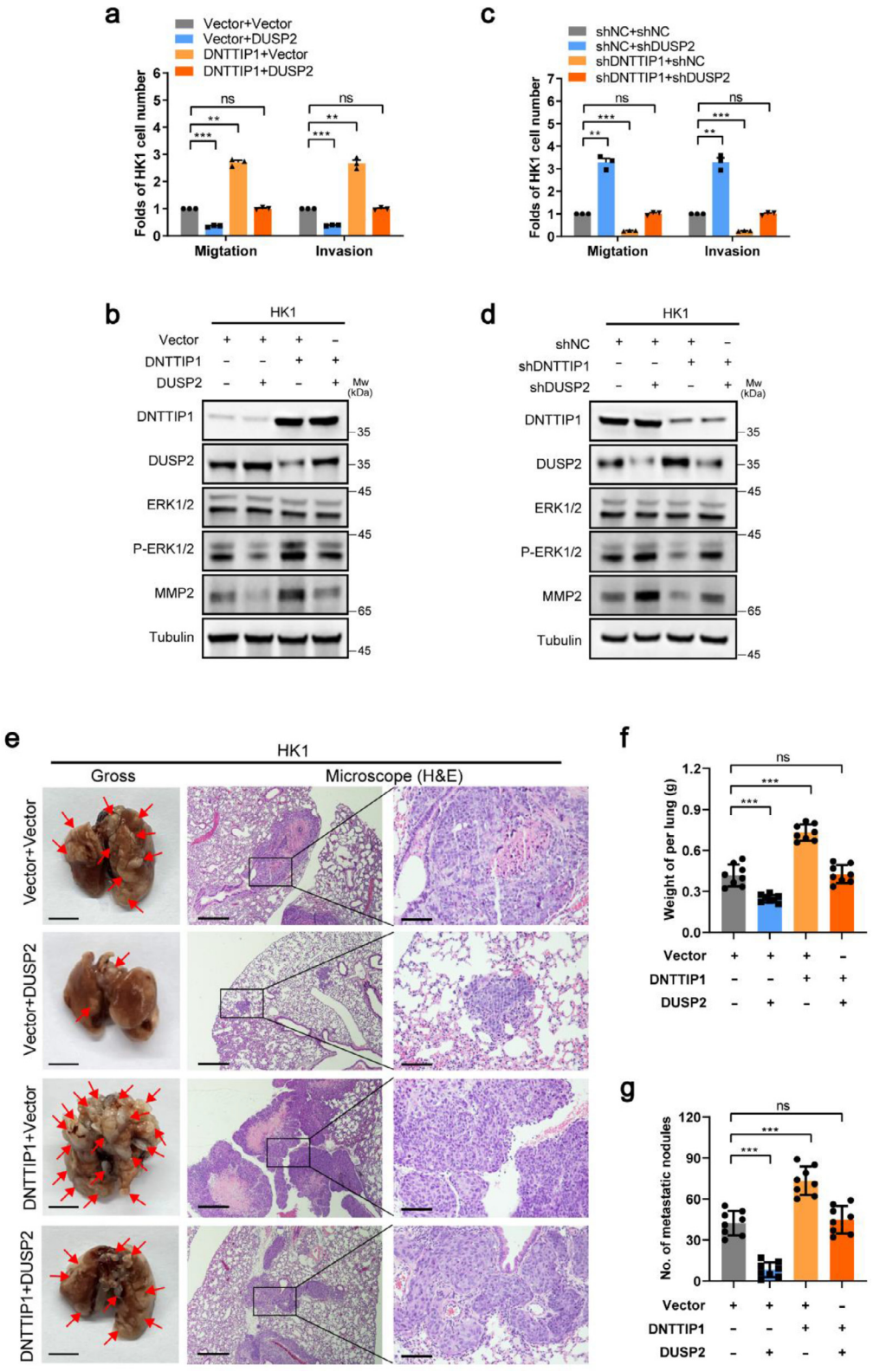

Figure 6. The effect of DNTTIP1 on NPC metastasis depends on DUSP2. (a, c) Migration and invasion abilities were determined using the indicated stable cells. Representative data of three independent experiments. Data are represented as the mean ± SD.

variety of tumors. For example, the combination of Chidamide with PD-1 blocker may improve the efficacy of soft tissue sarcoma and triple-negative breast cancer[32,33]; Chidamide increases the sensitivity of acute myeloid leukemia cells to anthracyclines by inhibiting the HDAC3-Akt-P21-CDK2 signaling pathway.[34] Although recent clinical studies have identified gemcitabine in combination with cisplatin as the standard first-line therapy for recurrent or metastatic NPC, there is still a lack of targeted treatment options for NPC.[35] Previous studies have found that HDAC4 inhibitor Tasquinimod suppresses NPC cell migration and invasion by regulating EMT.[36] SAHA, FK228, and Romidepsin suppress NPC proliferation *in vitro* and *in vivo*.[37-39] Abexinostat has synergistic cytotoxic effects in combination with cisplatin or irradiation in the *in vitro* NPC model.[40] In addition, the combination of proteasome inhibitor Bortezomib, and class I HDAC inhibitors MS-275, Apicidin, or Romidepsin, effectively promotes apoptosis of NPC cells *in vivo* and *in vitro*.[41] These results suggest that HDAC inhibitors have a promising application in the treatment of NPC. However, little study has been done on the role of HDAC inhibitors in NPC metastasis *in vivo*. In our study, we demonstrated that Chidamide treatment significantly decreased DNTTIP1 expression level *in vitro* and *in vivo*. Furthermore, the promoting effect of DNTTIP1/HDAC1 on cell migration, invasion, and metastasis was eliminated by Chidamide. This study provides evidence both at the cellular level and in an animal model to prove that Chidamide has potential transformational value in NPC treatment by targeting the DNTTIP1/HDAC1-DUSP2 axis. Thus, the combination of Chidamide with chemotherapeutic agents or immunosuppressants has potential clinical application value in the treatment of NPC. As we know, HDACs are ubiquitously expressed in different types of cancer and can participate in multiple epigenetic regulating complexes. In addition to HDAC1, the scaffold protein DNTTIP1, which determines the specificity of the MiDAC complex, also determines the DNA regions to which the complex binds to[13]. Therefore, the down-regulation of DNTTIP1 expression by Chidamide treatment regulates the specific gene and reduces the suppression of the MiDAC complex on the *DUSP2* promoter. According to this result, we speculated that Chidamide may affect the protein level of DNTTIP1 through inhibiting HDACs and upregulating the acetylation level. This hypothesis needs to be further studied.

Aberrant activation of the ERK pathway is involved in the progression of a variety of tumors and affects several cellular processes such as cell proliferation, cell survival, and metastasis.[42-45] DUSP2 primarily functions to inactivate ERK via direct dephosphorylation of threonine and tyrosine residues.[46,47] In fact, the lack of DUSP2 expression and the activation of ERK signal has been proved in many types of cancer, however, the molecular mechanism is not clear.[20] Here, we demonstrated that DNTTIP1 mediated the MiDAC complex to exert a highly processive deacetylation effect on the *DUSP2* promoter, impairing DUSP2 transcription and greatly activating ERK signaling pathway. Furthermore, targeting DNTTIP1/HDAC1 by Chidamide resulted in down-regulation of ERK signaling and decreased MMP2 level through up-regulating DUSP2. A recent study also demonstrates that DUSP2-regulated genes are similar to those controlled by HDACs and that treatment with HDAC inhibitors eliminates cancer stemness, tumor growth, and drug resistance caused by DUSP2 downregulation.[48]

In summary, our studies shed new light on the oncogenic role of DNTTIP1 in NPC, and DNTTIP1 may become a new marker for NPC patients to predict clinical outcomes. Although the detail of the strategy that targets the DNTTIP1/HDAC1-DUSP2-ERK signaling axis requires further investigation, it may benefit patients with NPC.

Contributors

Shirong Ding: Conceptualization, Data Curation, Methodology, Formal analysis, Investigation, Writing, Visualization. Ying Gao: Data Curation, Methodology, Formal analysis, Investigation, Visualization. Dongming Lv: Methodology, Formal analysis, Investigation, Visualization. Yalan Tao: Methodology, Resources. Songran Liu: Methodology, Visualization, Resources. Chen Chen: Methodology, Resources. Zilu Huang: Data Curation, Validation. Shuohan Zheng: Data Curation, Validation. Yujun Hu: Data Curation, Validation. Larry Ka-Yue Chow: Resources. Yinghong Wei: Data Curation, Validation. Ping Feng: Data Curation, Validation. Wei Dai: Resources. Xin Wang: Conceptualization, Methodology, Formal analysis, Investigation, Writing, Visualization. Yunfei Xia: Conceptualization, Supervision, Project administration, Resources, Funding acquisition, Editing. All authors read and approved the final version of the manuscript.

* $p < 0.05$, ** $p < 0.01$, *** $p < 0.001$, ns, no significance using Student's *t*-test. **(b, d)** The indicated proteins were analyzed by Western blotting in the indicated stable cells. Western Blot bands were derived from three separate experiments but only one representative loading control is shown. **(e-g)** The indicated cells were injected into the tail vein of BALB/c nude mice to construct a lung metastasis model (n=8 per group). General views (left, scale bar: 5mm) and H&E staining of lung tissues of the mouse models with the indicated cells (middle, scale bar: 500μm; right, scale bar: 100μm). The red arrows indicate macroscopic pulmonary nodules **(e)**. Lung weight **(f)**, and quantification of macroscopic metastatic nodules **(g)**. Data are represented as the mean ± SD. *** $p < 0.001$, ns, no significance using Student's *t*-test.

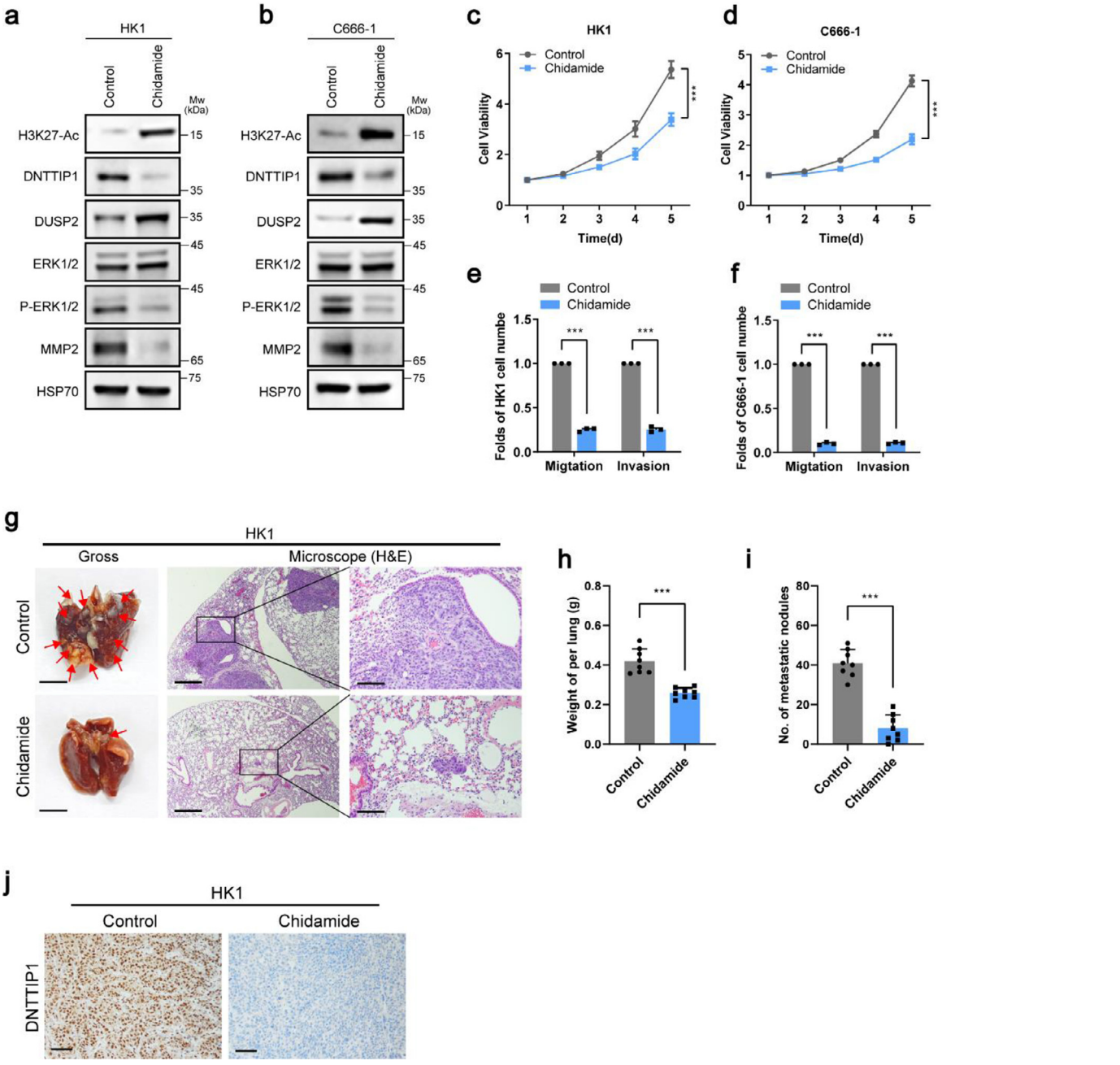

Figure 7. Chidamide inhibits cell migration, invasion, and metastasis of NPC. (a-b) HK1 and C666-1 cells were exposed to 1 μM Chidamide for 24 hours. The indicated proteins were analyzed by Western blotting in the indicated cells of three independent experiments. **(c-d)** Cell proliferation of HK1 and C666-1 cells when exposed to control or Chidamide. Representative data of three independent experiments. Data are represented as the mean ± SD. *** $p < 0.001$ using Student's *t*-test. **(e-f)** Migration and invasion abilities were determined using the indicated cells. Representative data of three independent experiments. Data are represented as the mean ± SD. *** $p < 0.001$ using Student's *t*-test. **(g-i)** HK1 cells were injected into the tail vein of BALB/c nude mice to construct a lung metastasis model and treated with Chidamide or vehicle (n=8 per group). General views (left, scale bar: 5mm) and H&E staining of lung tissues of the mouse models with the indicated cells (middle, scale bar: 500μm; right, scale bar: 100μm). The red arrows indicate macroscopic pulmonary nodules **(g)**. Lung weight **(h)**, and quantification of macroscopic metastatic nodules **(i)**. Data are represented as the mean ± SD. ** $p < 0.01$, *** $p < 0.001$ using Student's *t*-test. **(j)** IHC of the xenografted tumors shows decreased level for DNTTIP1 in the Chidamide-treated group. These results are repeated in three independent experiments. Scale bar: 100μm.

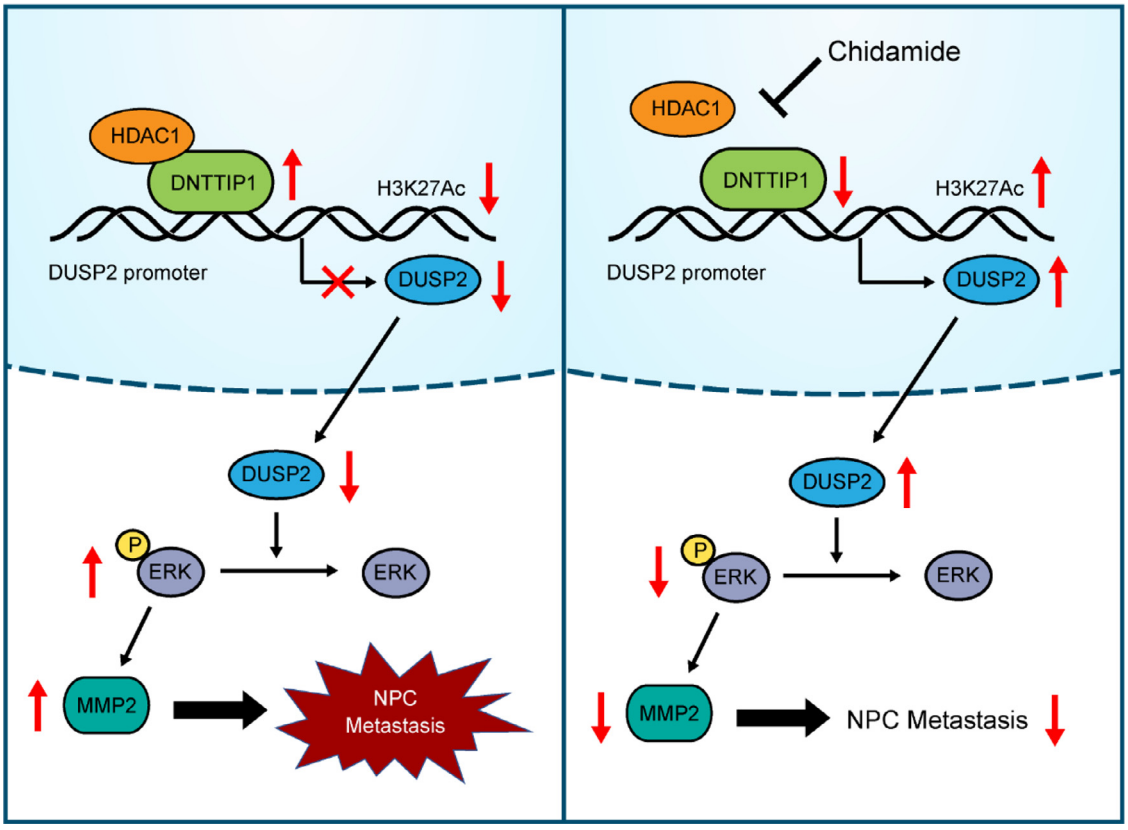

Figure 8. A proposed model of the biological function of DNTTTIP1 in nasopharyngeal carcinoma. DNTTIP1 could silence *DUSP2* gene expression by recruiting HDAC1 to *DUSP2* promoter and maintaining a deacetylated state of histone H3K27. Downregulation of DUSP2 resulted in aberrant activation of the ERK signaling and elevated MMP2 levels, promoting NPC metastasis. Furthermore, the HDAC inhibitor Chidamide could suppress NPC metastasis via regulating the DNTTIP1/HDAC1-DUSP2 axis.

Declaration of interests

Authors declare that they have no competing interests.

Data sharing statement

The RNA sequencing data has been uploaded to NCBI's SRA, accession to cite for the SRA data: PRJNA815737 and PRJNA812888.

Acknowledgements

This work was supported by the National Nature Science Foundation in China (NSFC) (Grants 81872464, 82073243).

Supplementary materials

Supplementary material associated with this article can be found in the online version at doi:10.1016/j.ebiom.2022.104100.

References

1 Wong KCW, Hui EP, Lo KW, et al. Nasopharyngeal carcinoma: an evolving paradigm. *Nat Rev Clin Oncol*. 2021;18(11):679–695.
2 Mai HQ, Chen QY, Chen D, et al. Toripalimab or placebo plus chemotherapy as first-line treatment in advanced nasopharyngeal carcinoma: a multicenter randomized phase 3 trial. *Nat Med*. 2021;27(9):1536–1543.
3 Sidaway P. Chemoradiotherapy improves NPC outcomes. *Nat Rev Clin Oncol*. 2020;17(10):592.
4 Hong S, Zhang Y, Yu G, et al. Gemcitabine plus cisplatin versus fluorouracil plus cisplatin as first-line therapy for recurrent or metastatic nasopharyngeal carcinoma: final overall survival analysis of GEM20110714 phase III study. *J Clin Oncol*. 2021;39(29):3273–3282.
5 Yang Y, Qu S, Li J, et al. Camrelizumab versus placebo in combination with gemcitabine and cisplatin as first-line treatment for recurrent or metastatic nasopharyngeal carcinoma (CAPTAIN-1st): a multicentre, randomised, double-blind, phase 3 trial. *Lancet Oncol*. 2021;22(8):1162–1174.
6 Huang CL, Guo R, Li JY, et al. Nasopharyngeal carcinoma treated with intensity-modulated radiotherapy: clinical outcomes and patterns of failure among subsets of 8th AJCC stage IVa. *Eur Radiol*. 2020;30(2):816–822.
7 Li ZQ, Xia YF, Liu Q, et al. Radiotherapy-related typing in 842 patients in canton with nasopharyngeal carcinoma. *Int J Radiat Oncol Biol Phys*. 2006;66(4):1011–1016.
8 Chen YP, Ismaila N, Chua MLK, et al. Chemotherapy in combination with radiotherapy for definitive-intent treatment of stage II-

IVA nasopharyngeal carcinoma: CSCO and ASCO guideline. *J Clin Oncol*. 2021;39(7):840–859.
9 Yamashita N, Shimazaki N, Ibe S, et al. Terminal deoxynucleotidyltransferase directly interacts with a novel nuclear protein that is homologous to p65. *Genes Cells*. 2001;6(7):641–652.
10 Hayano T, Koiwai K, Ishii H, et al. TdT interacting factor 1 enhances TdT ubiquitylation through recruitment of BPOZ-2 into nucleus from cytoplasm. *Genes Cells*. 2009;14(12):1415–1427.
11 Bantscheff M, Hopf C, Savitski MM, et al. Chemoproteomics profiling of HDAC inhibitors reveals selective targeting of HDAC complexes. *Nat Biotechnol*. 2011;29(3):255–265.
12 Pagliuca FW, Collins MO, Lichawska A, Zegerman P, Choudhary JS. Pines J. Quantitative proteomics reveals the basis for the biochemical specificity of the cell-cycle machinery. *Mol Cell*. 2011;43(3):406–417.
13 Turnbull RE, Fairall L, Saleh A, et al. The MiDAC histone deacetylase complex is essential for embryonic development and has a unique multivalent structure. *Nat Commun*. 2020;11(1):3252.
14 Zhang Y, Wang Z, Huang Y, et al. TdIF1: a putative oncogene in NSCLC tumor progression. *Signal Transd Target Ther*. 2018;3(1).
15 Sawai Y, Kasamatsu A, Nakashima D, et al. Critical role of deoxynucleotidyl transferase terminal interacting protein 1 in oral cancer. *Lab Invest*. 2018;98(8):980–988.
16 Xu JL, Guo Y. A comprehensive analysis of different gene classes in pancreatic cancer: SIGLEC15 may be a promising immunotherapeutic target. *Invest New Drugs*. 2021.
17 Lv D, Ding S, Zhong L, et al. M(6)A demethylase FTO-mediated downregulation of DACT1 mRNA stability promotes Wnt signaling to facilitate osteosarcoma progression. *Oncogene*. 2022;41(12):1727–1741.
18 Ding S, Wang X, Lv D, et al. EBF3 reactivation by inhibiting the EGR1/EZH2/HDAC9 complex promotes metastasis via transcriptionally enhancing vimentin in nasopharyngeal carcinoma. *Cancer Lett*. 2022;527:49–65.
19 Mondal B, Jin H, Kallappagoudar S, et al. The histone deacetylase complex MiDAC regulates a neurodevelopmental gene expression program to control neurite outgrowth. *Elife*. 2020;9.
20 Wang CA, Li CF, Huang RC, Li YH, Liou JP, Tsai SJ. Suppression of extracellular vesicle VEGF-C-mediated lymphangiogenesis and pancreatic cancer early dissemination by a selective HDAC1/2 inhibitor. *Mol Cancer Ther*. 2021;20(9):1550–1560.
21 Keyse SM. Dual-specificity MAP kinase phosphatases (MKPs) and cancer. *Cancer Metastasis Rev*. 2008;27(2):253–261.
22 Shi Y, Dong M, Hong X, et al. Results from a multicenter, open-label, pivotal phase II study of chidamide in relapsed or refractory peripheral T-cell lymphoma. *Ann Oncol*. 2015;26(8):1766–1771.
23 Jiang Z, Li W, Hu X, et al. Tucidinostat plus exemestane for postmenopausal patients with advanced, hormone receptor-positive breast cancer (ACE): a randomised, double-blind, placebo-controlled, phase 3 trial. *Lancet Oncol*. 2019;20(6):806–815.
24 Wu SE, Hashimoto-Hill S, Woo V, et al. Microbiota-derived metabolite promotes HDAC3 activity in the gut. *Nature*. 2020;586(7827):108–112.
25 Baretti M, Yarchoan M. Epigenetic modifiers synergize with immune-checkpoint blockade to enhance long-lasting antitumor efficacy. *J Clin Invest*. 2021;131(16).
26 Yan B, Yang J, Kim MY, et al. HDAC1 is required for GATA-1 transcription activity, global chromatin occupancy and hematopoiesis. *Nucleic Acids Res*. 2021;49(17):9783–9798.
27 Chagraoui J, Girard S, Spinella JF, et al. UM171 preserves epigenetic marks that are reduced in ex vivo culture of human HSCs via potentiation of the CLR3-KBTBD4 complex. *Cell Stem Cell*. 2021;28(1):48–62. e6.
28 Gouridis G, Muthahari YA, de Boer M, et al. Structural dynamics in the evolution of a bilobed protein scaffold. *Proc Natl Acad Sci U S A*. 2021;118(49).
29 Cha HJ, Uyan O, Kai Y, et al. Inner nuclear protein Matrin-3 coordinates cell differentiation by stabilizing chromatin architecture. *Nat Commun*. 2021;12(1):6241.
30 Itoh T, Fairall L, Muskett FW, et al. Structural and functional characterization of a cell cycle associated HDAC1/2 complex reveals the structural basis for complex assembly and nucleosome targeting. *Nucleic Acids Res*. 2015;43(4):2033–2044.
31 Werbeck ND, Shukla VK, Kunze MBA, et al. A distal regulatory region of a class I human histone deacetylase. *Nat Commun*. 2020;11(1):3841.
32 Que Y, Zhang XL, Liu ZX, et al. Frequent amplification of HDAC genes and efficacy of HDAC inhibitor chidamide and PD-1 blockade combination in soft tissue sarcoma. *J Immunother Cancer*. 2021;9(2).
33 Tu K, Yu Y, Wang Y, et al. Combination of chidamide-mediated epigenetic modulation with immunotherapy: boosting tumor immunogenicity and response to PD-1/PD-L1 blockade. *ACS Appl Mater Interfaces*. 2021;13(33):39003–39017.
34 Wang H, Liu YC, Zhu CY, et al. Chidamide increases the sensitivity of refractory or relapsed acute myeloid leukemia cells to anthracyclines via regulation of the HDAC3 -AKT-P21-CDK2 signaling pathway. *J Exp Clin Cancer Res*. 2020;39(1):278.
35 Zhang L, Huang Y, Hong S, et al. Gemcitabine plus cisplatin versus fluorouracil plus cisplatin in recurrent or metastatic nasopharyngeal carcinoma: a multicentre, randomised, open-label, phase 3 trial. *Lancet*. 2016;388(10054):1883–1892.
36 Cheng C, Yang J, Li SW, et al. HDAC4 promotes nasopharyngeal carcinoma progression and serves as a therapeutic target. *Cell Death Dis*. 2021;12(2):137.
37 Xie J, Wang Z, Fan W, et al. Targeting cancer cell plasticity by HDAC inhibition to reverse EBV-induced dedifferentiation in nasopharyngeal carcinoma. *Signal Transd Target Ther*. 2021;6(1):333.
38 Hui KF, Ho DN, Tsang CM, Middeldorp JM, Tsao GS, Chiang AK. Activation of lytic cycle of Epstein-Barr virus by suberoylanilide hydroxamic acid leads to apoptosis and tumor growth suppression of nasopharyngeal carcinoma. *Int J Cancer*. 2012;131(8):1930–1940.
39 Hui KF, Cheung AK, Choi CK, et al. Inhibition of class I histone deacetylases by romidepsin potently induces Epstein-Barr virus lytic cycle and mediates enhanced cell death with ganciclovir. *Int J Cancer*. 2016;138(1):125–136.
40 Gressette M, Verillaud B, Jimenez-Pailhes AS, et al. Treatment of nasopharyngeal carcinoma cells with the histone-deacetylase inhibitor abexinostat: cooperative effects with cis-platin and radiotherapy on patient-derived xenografts. *PLoS One*. 2014;9(3):e91325.
41 Hui KF, Chiang AK. Combination of proteasome and class I HDAC inhibitors induces apoptosis of NPC cells through an HDAC6-independent ER stress-induced mechanism. *Int J Cancer*. 2014;135(12):2950–2961.
42 Ponsioen B, Post JB, Buissant des Amorie JR, et al. Quantifying single-cell ERK dynamics in colorectal cancer organoids reveals EGFR as an amplifier of oncogenic MAPK pathway signalling. *Nat Cell Biol*. 2021;23(4):377–390.
43 Hong A, Piva M, Liu S, et al. durable suppression of acquired MEK inhibitor resistance in cancer by sequestering MEK from ERK and promoting antitumor T-cell immunity. *Cancer Discov*. 2021;11(3):714–735.
44 Zhu G, Herlyn M, Yang X. TRIM15 and CYLD regulate ERK activation via lysine-63-linked polyubiquitination. *Nat Cell Biol*. 2021;23(9):978–991.
45 Gagliardi PA, Dobrzynski M, Jacques MA, et al. Collective ERK/Akt activity waves orchestrate epithelial homeostasis by driving apoptosis-induced survival. *Dev Cell*. 2021;56(12):1712–1726. e6.
46 Rohan PJ, Davis P, Moskaluk CA, et al. PAC-1: a mitogen-induced nuclear protein tyrosine phosphatase. *Science*. 1993;259(5102):1763–1766.
47 Owens DM, Keyse SM. Differential regulation of MAP kinase signalling by dual-specificity protein phosphatases. *Oncogene*. 2007;26(22):3203–3213.
48 Hou PC, Li YH, Lin SC, et al. Hypoxia-induced downregulation of DUSP-2 phosphatase drives colon cancer stemness. *Cancer Res*. 2017;77(16):4305–4316.